中国科学 地球科学

SCIENCE CHINA Earth Sciences

ISSN 1674-7313
CN 11-5843/P
中国科学: 地球科学(英文版)

Earth Sciences

Volume 62 · Number 6
June 2019

SCIENCE CHINA PRESS
Springer
Chinese Academy of Sciences
National Natural Science Foundation of China

SCIENCE CHINA Earth Sciences

Vol. 62 No. 6 Jun. 2019 891–000

SCIENCE CHINA
Earth Sciences

•PROGRESS•

June 2019 Vol.62 No.6: 891–908
https://doi.org/10.1007/s11430-018-9317-8

Impact of oceans on climate change in drylands

Xiaodan GUAN[1], Jieru MA[1], Jianping HUANG[1*], Ruixin HUANG[2,3], Lei ZHANG[1] & Zhuguo MA[4]

[1] *Key Laboratory for Semi-Arid Climate Change of the Ministry of Education, College of Atmospheric Sciences, Lanzhou University, Lanzhou 730000, China;*
[2] *Woods Hole Oceanographic Institution, Woods Hole MA 02543, USA;*
[3] *State Key Laboratory of Tropical Oceanography, South China Sea Institute of Oceanology, Chinese Academy of Sciences, Guangzhou 510301, China;*
[4] *Key Laboratory of Regional Climate-Environment for Temperate East Asia, Institute of Atmospheric Physics, Chinese Academy of Sciences, Beijing 100029, China*

Received August 16, 2018; revised October 24, 2018; accepted December 7, 2018; published online March 6, 2019

Abstract Drylands account for approximately 41% of the global total land area. Significant warming and rare precipitation in drylands result in a fragile ecology and deterioration of the living environment, making it more sensitive to global climate change. As an important regulator of the Earth's climate system, the oceans play a vital role in the process of climate change in drylands. In modern climate change in particular, the impact of marine activities on climate change in drylands cannot be neglected. This paper reviews the characteristics of climate change in drylands over the past 100 years, and summarizes the researches conducted on the impact of marine activities on these changes. The review focuses on the impact of the Pacific Decadal Oscillation (PDO), Atlantic Multidecadal Oscillation (AMO), El Niño and La Niña on climate change in drylands, and introduces the mechanisms by which different oceanic oscillation factors synergistically affect climate change in drylands. Studies have shown that global drylands have experienced a significant intensification in warming in the past 100 years, which shows obvious characteristics of interdecadal dry/wet variations. The characteristics of these changes are closely related to the oscillatory factors of the oceanic interdecadal scale. Different phase combinations of oceanic oscillation factors significantly change the land-sea thermal contrast, which in turn affects the westerly jet, planetary wave and blocking frequency, resulting in changes in the temperature and dry/wet characteristics of drylands. With the intensification of climate change in drylands, the impact of marine activities on these regions will reveal new characteristics in the future, which will increase the uncertainty of future climate change in drylands and intensify the impact of these drylands on global climate.

Citation: Guan X, Ma J, Huang J, Huang R, Zhang L, Ma Z. 2019. Impact of oceans on climate change in drylands. Science China Earth Sciences, 62: 891–908, https://doi.org/10.1007/s11430-018-9317-8

1. Introduction

The terms drylands refer to regions in which the annual precipitation (P) is much smaller than the annual potential evapotranspiration (PET). Regions with an aridity index (AI) of less than 0.65 are usually classified as being drylands (Hulme, 1996; Feng and Fu, 2013; Huang et al., 2016), and include hyper-arid, arid, semi-arid and dry sub-humid regions (Feng and Fu, 2013; Spinoni et al., 2015). Drylands account for approximately 41% of the global total land region (White and Nackoney, 2003), and accommodate more than 38% of the global population (Reynolds et al., 2007), with 90% of these being located in developing countries (GLP, 2005; Armah et al., 2010; Huang et al., 2017a). These drylands face many problems, such as large populations and low soil fertility, which make them extremely sensitive to

* Corresponding author (email: hjp@lzu.edu.cn)

global changes caused by climate warming and human activities (Scheffer et al., 2001; Rietkerk et al., 2004; Maestre et al., 2013; Li et al., 2016; Zhou et al., 2016). In the process of modern climate change, the warming of drylands is the most significant (Huang et al., 2012, 2017b), and historical observations and model simulations have both indicated that the global drylands have continuously expanded over the past 60 years and that this expansion will accelerate during the 21st century (Huang et al., 2017c). Climate warming, drought aggravation and population growth will increase the risk of desertification in developing countries. The expansion of land desertification caused by climate change and human activities will cause a further decline in land productivity, population migration, and deterioration of the ecological environment, which will have a profound impact on the social economy. Therefore, understanding the characteristics of climate change in global drylands is essential for delaying desertification, protecting renewable regional resources and developing reasonable policies.

Climate change in drylands is the result of multifactorial effects, it is affected not only by natural factors such as ocean activities and atmospheric circulation, but also by human factors such as greenhouse gases and changes in land-use. Oceans are an important part of the earth's climate system, and studying the impact of oceans on climate change in drylands is an important part of understanding climate change and its mechanism in drylands. Previous studies have shown that oceanic activities, especially sea surface temperature (SST) in the Pacific, Atlantic and Indian Ocean Basin, can affect the precipitation, temperature, and dry and wet changes in global drylands at different time scales (Hu et al., 2018; Wang et al., 2018; Fu and Ma, 2008). The interaction between the ocean and the atmosphere determines the global dry and wet changes on the interdecadal scale (Guan et al., 2017). In addition, a large number of studies have investigated the impact of oceans on climate change in drylands from the perspective of different phase changes and the combination of oceanic oscillation factors, as well as the land-sea thermal contrast (Huang et al., 2017a, 2017b). However, there are still many unresolved issues, such as how the interaction between different sea areas affects climate change in drylands, and how to quantify the relative contribution of marine activities to climate evolution in drylands and the resulting response processes. Based on previous research conducted in China and across the world, this paper systematically summarizes the latest progress concerning the impact of oceans on climate change in drylands during modern climate change, and discusses the future development trends with the aim of fully understanding the mechanisms of climate change and preventing desertification in drylands. The possible impacts of marine activities on desertification is evaluated in order to provide a scientific basis for the prevention of further desertification, the hazards of mitigating sandstorms, and developing countermeasures to adapt to and mitigate global climate change.

2. Characteristics of climate change in drylands

As an important part of global land, drylands play an indispensable role in the process of global climate change. In the context of global warming in recent decades, drylands have continuously expanded (Huang et al., 2016, 2017c), and frequent extreme droughts have occurred. At the same time, the interdecadal signals of climate change have also caused significant interdecadal characteristics in semi-arid regions, for example, during the rapid warming period during the 1980s in the northern hemisphere (NH) and the warming slowdown period in the early 21st century, the climate in semi-arid regions showed significant interdecadal variation characteristics. In terms of the characteristics of climate change in semi-arid regions in the future, studies have shown that the forecasted expansion of semi-arid regions in future scenarios has been obviously underestimated, and that there are prominent uncertainties in the climate change characteristics of semi-arid regions in future scenarios.

2.1 Distribution and evolution of modern drylands

The global drylands are mainly distributed in the middle and low latitude regions of the NH (Figure 1). Hyper-arid regions (AI≤0.05) are concentrated in the central and northern parts of the Sahara Desert, the Rubal-Khali Desert in the eastern Arabian Peninsula, the Taklimakan Desert in northwestern China, and the Atacama Desert; arid regions (0.05≤AI<0.2) are mainly located in the southern Sahara Desert, southern Africa, Western Arabian Peninsula, Central Asia, Mongolia and northern China, and most regions in Australia; semi-arid (0.2≤AI<0.5) and dry sub-humid (0.5≤AI<0.65) regions are mainly located in the western United States, the west coast of South America, Central and East Asia, and most regions of Central Australia except for the desert areas.

The total area of the drylands has continuously expanded during the past six decades (see Figure 2). The range of hyper-arid, arid, semi-arid and dry sub-humid regions increased by 0.6×10^6, 0.1×10^6, 1.6×10^6 and 0.5×10^6 km^2, respectively (Figure 2). Among these, the largest area expansion occurred in the semi-arid regions. The expansion of semi-arid regions accounted for more than half of the total drylands expansion since the early 1960s (Figure 2c). Before the 1980s, the total area of dry sub-humid regions was almost constant, and decreased in the early 1980s before expanding significantly in the late 1980s (Figure 2b). The total area of the arid regions showed strong interdecadal oscillations, with a weak decreased during the 1970s. The area recovered in the early 1980s, and during the period of 1990–2004 it was

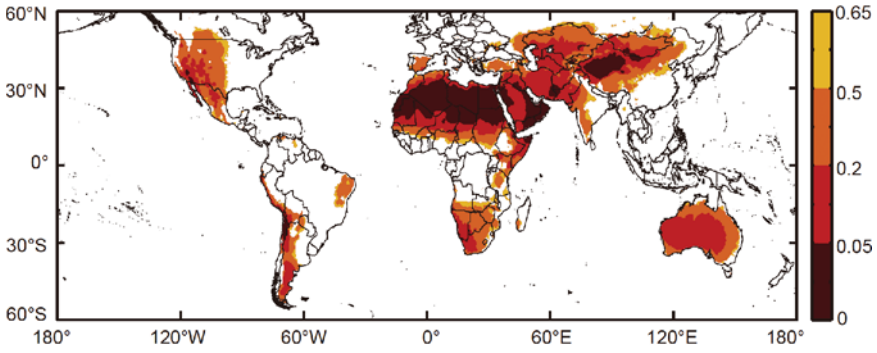

Figure 1 Global distribution of drylands based on the aridity index (AI) for 1961–1990 climatology. Cited from Feng and Fu (2013).

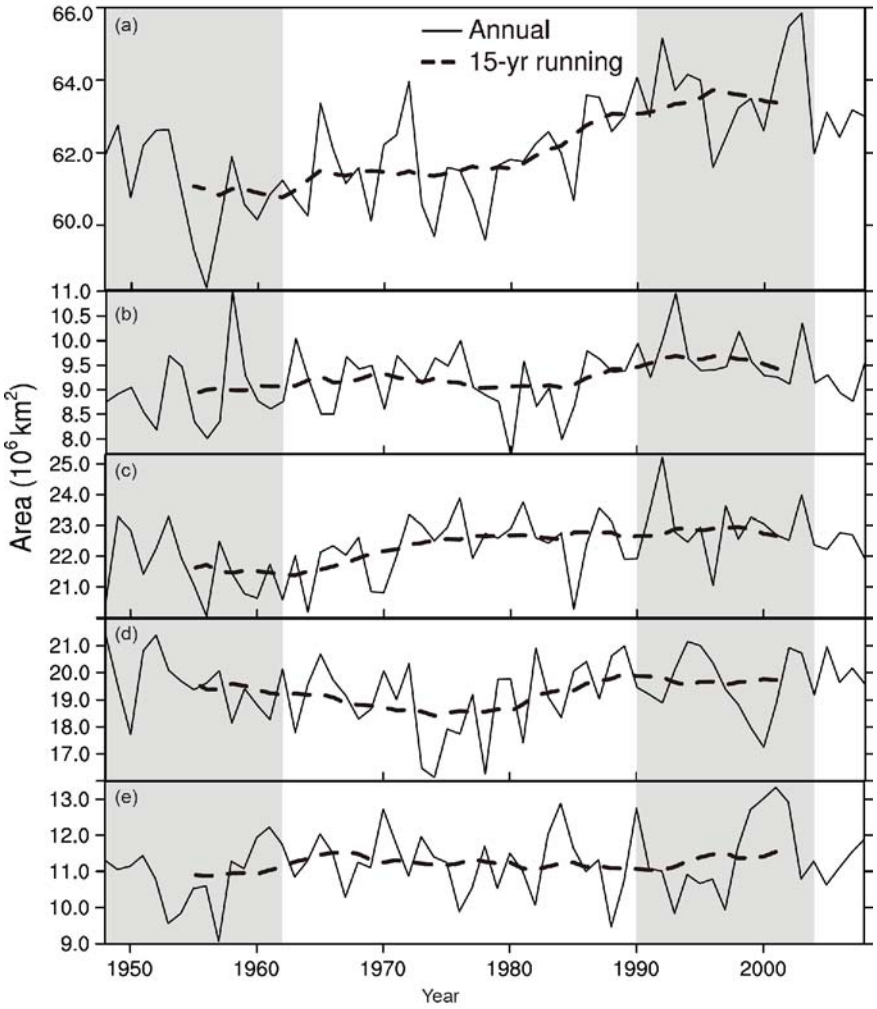

Figure 2 Temporal variations in the area (10^6 km^2) of total drylands (a); dry sub-humid region (b); semi-arid region (c); arid region (d); and hyper-arid region (e) during 1948–2008. The dashed line is the 15-year running mean. Cited from Huang et al. (2016).

comparable to the area before the 1970s (Figure 2d). Owing to the large-scale precipitation anomalies in the southern hemisphere in the 1970s, the area of arid regions was decreased, resulting in the increase in area of the semi-arid regions (Feng and Fu, 2013).

According to the results from Huang et al. (2016), distribution of the drylands is not fixed, and undergoes dynamic changes (Figure 3). The transition from a dry sub-humid (semi-arid) to a semi-arid (arid) region occurs mainly in East Asia, East Australia, northern and southern Africa. The transition from a semi-arid (arid) to sub-humid/humid region mainly occurs in central/western Australia, central United

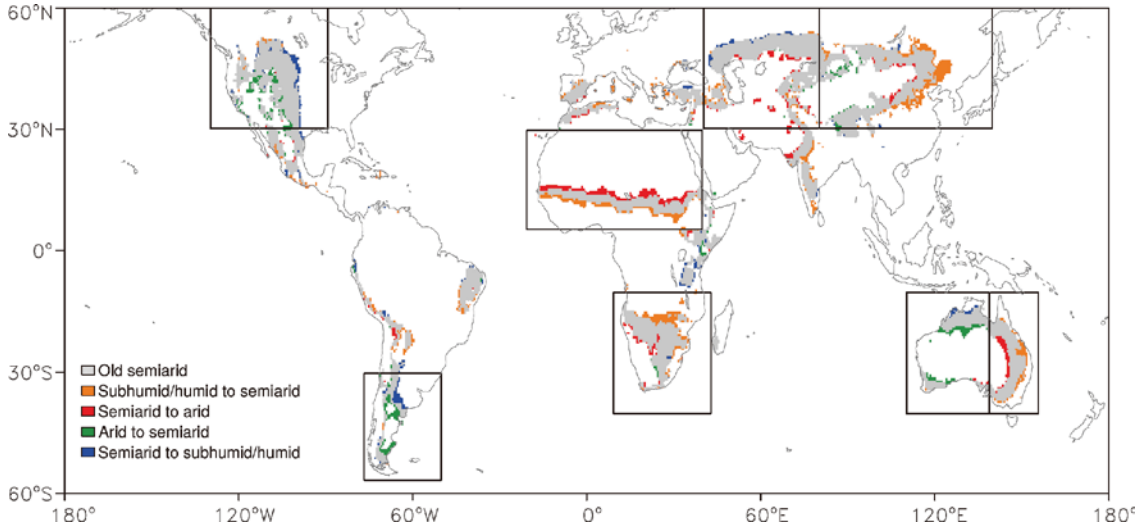

Figure 3 Global distribution of the semi-arid regions and the spatial distribution of their transitions that experienced a change in the climate classifications during 1990–2004 relative to 1948–1962. Cited form Huang et al. (2016).

States and southern South America. The results show that, except for central/western Australia, the eastern hemisphere is mainly become dry, while the mid-latitude regions in North America and South America become wet. In addition, the two temperate semi-arid regions in North America and East Asia show different variation characteristics. Drylands in North America become wetter, while semi-arid and dry sub-humid regions in Asia becoming drier. In addition, this aridification trend is evident in river flow records and in the observed Palmer Drought Severity Index (PDSI), which are consistent with changes in the AI (Dai and Zhao, 2017). The increase in the area of the global drylands is mainly caused by aridification in Africa, southern Europe, East Asia and eastern Australia (Dai, 2011a, 2011b, 2013a; Dai and Zhao, 2017; Huang et al., 2017c; Fu and Mao, 2017). This aridification trend is largely related to the reduction in precipitation caused by the interdecadal oscillations of the Pacific Ocean and the rapid warming that has occurred since the 1980s (Dai, 2013a; Dai and Zhao, 2017).

2.2 Characteristics of temperature change: enhanced warming

As a special component of global land, drylands have an important impact on global climate change. In the context of global warming, drylands have shown the most significant warming in the past 100 years; at the same time, there have been significant regional differences between climate changes in different drylands. Huang et al. (2012) found that temperature increases in the whole year, the warm season, and the cold season in the mid-high latitude regions of the NH during 1901–2009 were 1.33, 0.85 and 1.89°C, respectively. The temperature increases in the warm season of semi-arid regions in the mid-high latitudes of Europe, Asia, and North America were 0.95, 0.68 and 1.05°C, respectively, and the warming in the semi-arid regions of North America was greater than that was in Asia. The temperature increase in the cold season was 1.41, 2.42 and 1.50°C, respectively, and the warming in the semi-arid region of Asia was greater than that of the semi-arid region in North America, showing the most significant warming trend. After further quantification of the contribution of the warming in the drylands in the mid-high latitudes of the NH to global warming (Figure 4), it was found that the warming in the drylands contributes to almost 60% of global warming, whereas the drylands in Europe, Asia and North America contribute 8.76%, 5.65% and 0.64%, respectively, to global warming. Furthermore, the semi-arid regions contributed 6.29%, 13.81% and 6.85%, respectively, to global warming, and the semi-arid regions in Asia had the largest contribution to global warming (Table 1).

2.3 Characteristics of precipitation change at the interdecadal scale in typical drylands

Although the cause of global warming is still controversial, the fact that the temperature has increased in the past 100 years is undeniable (IPCC, 2007, 2013). In the context of global warming there is another important indicator, the change of precipitation in drylands shows significant regional differences, and research on the characteristics and mechanisms of precipitation changes under global warming has also attracted significant attention (Lambert and Allen, 2009; Bichet et al., 2011; Dong and Dai, 2015). A large amount of research has shown that the drylands have become more and more dry in the past 100 years (Nicholson et al., 1998; Nicholson and Grist, 2001; Ma and Shao, 2006; Narisma et al., 2007). Owing to global warming, there are sig-

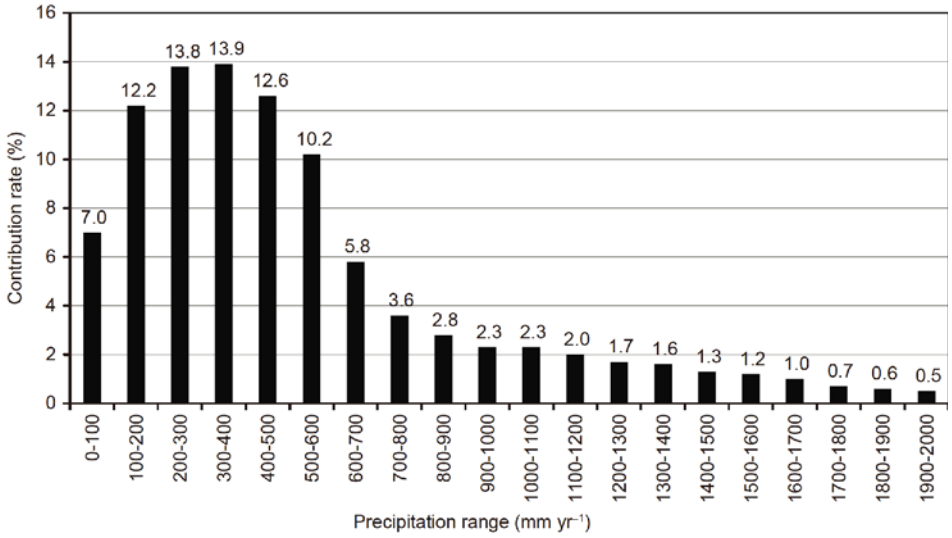

Figure 4 Regional contributions (%) of surface temperature trend in different precipitation ranges to global temperature trend for cold season during 1901–2009. Cited from Huang et al. (2012).

Table 1 Contribution of land-surface temperature trend in different mid-high latitude region to global temperature trend during 1901–2009 (%)[a)]

	Europe	Asia	North America
Arid	8.76	5.65	0.64
Semi-arid	6.29	13.81	6.85
Sub-humid	3.23	2.48	3.54
Humid	0.73	3.11	2.20

a) Cited from Huang et al. (2016)

nificant regional differences in the precipitation changes in drylands (Ma, 2007; Ault and George, 2010; Shi et al., 2002). Previous research has made meaningful progress in determining the changes in global and regional precipitation (Huang et al., 2011; Rasmusson and Arkin, 1993; Trenberth, 2011; Gu and Adler, 2013, 2015), but there is a lack of comparative studies on interdecadal variations in precipitation at different scales around the world. At the same time, the major drought events in the drylands in the past 100 years are mostly related to age-scale climate change. A lot of research has been carried out on climate changes at the chronological scale (Delworth and Manaba, 1993; Fu and Huang, 1996; Wang and Zhu, 1999; Li et al., 2002; Huang et al., 2006; Ma and Fu, 2007; Fu et al., 2008). Precipitation is the dominant factor in the formation of drought on the decadal scale and this is of great significance for the study of decadal climate in the drylands.

Figure 5 shows the interdecadal oscillations, trends, and interdecadal-scale synthetic precipitation changes for four typical representative regions in the drylands of North America, North China, North Africa, and Central Asia (Xu and Ma, 2017). The characteristics of evolution were analyzed to understand the evolution characteristics of precipitation and the regional differences at interdecadal scale in the typical drylands of the world. As shown in Figure 5, there are different interdecadal oscillation periods in the four typical regions. The interdecadal periods in North America and Central are both about 30 years, and the phases are basically the same. Both of these are rising trends, and they turned into wet periods in 1971 and 1975, respectively. The interdecadal periods in North China, North America and Central Asia are basically equal and the difference in the phases is not significant, but the long-term trend is reversed. It should be noted that, the phase and trend of the interdecadal period in North Africa is significantly different from those of the other three regions, which is also an important difference between North China and North Africa. Previous studies have discovered that long-term changes in North Africa and North China have similar characteristics (Yan et al., 1990; Ma and Fu, 2007), but the characteristics of the two regions in the interdecadal scale cannot be revealed owing to the limitations of the methods. As shown in Table 2, the drying trend in North China lasted for the longest period, which was 38 years, followed by North Africa (34 years) and North America (17 years). Although the duration of drying trend in Central Asia was the shortest, there have been two drying trends in the past 60 years. The duration of humidification is relatively short compared to aridification in Central Asia, but it occurs more frequently.

2.4 Characteristics of dry and wet changes and regional differences

A drying trend has been observed in the global drylands since 1950. The historically recorded precipitation, runoff and PDSI database of observations has also proved this trend. The drying of the global drylands is affected by ocean oscillation factors, dominated by global warming, and ex-

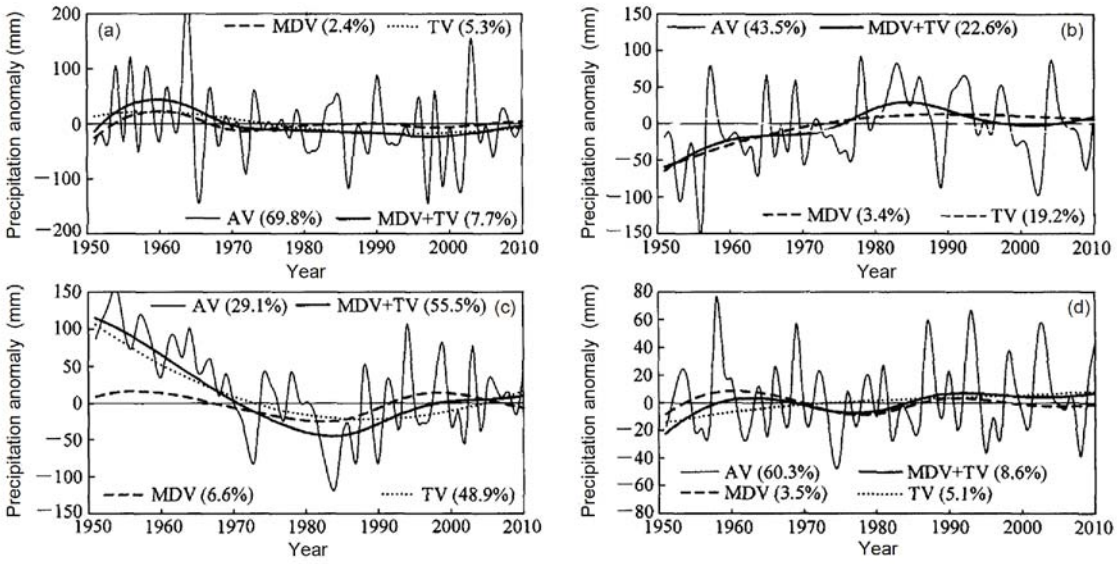

Figure 5 Multi-time scale variation characteristics of the average annual precipitation in four typical drylands of the world extracted using the Ensemble Empirical Mode Decomposition (EEMD) method. AV, MDV, and TV represent annual variability, multi-decadal variability, and trend variability, respectively; MDV+TV indicates multi-decadal change; numbers in brackets mean variance contributions. Cited from Xu and Ma (2017).

Table 2 The time statistics of trend and multi-decadal wet and dry oscillation of regional mean annual precipitation in typical drylands[a)]

		North America	North China	North Africa	Central Asia
Trend	Drought period	1985–2001	1961–1998	1951–1984	1964–1977 1993–2003
	Wet period	1951–1984 2001–2010	1951–1960 1999–2010	1985–2010	1951–1963 1978–1992
Interdecadal oscillation	Drought period	1951–1974	1970–2010	1969–2010	1951–1958 1969–1984
	Wet period	1975–2010	1952–1969	1951–1968	1959–1968 1985–2010

a) Cited from Xu and Ma (2017).

hibits different temporal and spatial characteristics in different drylands. From a global perspective, the land in the eastern hemisphere shows a drying trend and the land in America shows a wetting trend (Greve et al., 2014). Fu and Ma (2008) pointed out that the North American continent turned from dry to wet in the mid to late 1950s, while the African continent has turned from wet to dry since 1979, and the drought in Asia began in 1975. Huang et al. (2016) compared the new semi-arid regions which were transformed from other climate regions with the semi-arid regions that existed for many years. The analysis results indicated that the precipitation has decreased in the semi-arid regions of East Asia, but has increased in the semi-arid regions of North America. A PET increase has been observed in the semi-arid regions of East Asia, but a decrease has been found in the semi-arid regions of North America; the results of the AI were consistent with those for the precipitation. This indicates that the semi-arid regions in East Asia show a drying trend, and the semi-arid regions in North America show a wetting trend. Cai et al. (2012) proved that the semi-arid regions in the southern hemisphere, such as the south coast of Chile, South Africa and South Australia, have shown a drying trend in autumn since the late 1970s, especially during the period from April to May.

The drying of the drylands has resulted in a significant expansion of the global arid regions (Dai, 2011a, 2011b, 2013a; Dai and Zhao, 2017). Huang et al. (2016) analyzed the area change characteristics of the different climatic regions and found that most of the semi-arid regions showed an area expansion. Comparing the area of each semi-arid region in different time periods, it was found that the degree of aridification observed from 1990 to 2004 was more significant compared with the period from 1948 to 1962. The main reason for the expansion of aridification is the transi-

tion of humid and sub-humid regions to semi-arid regions, and the most significant aridification expansion occurred in East Asia, which contributed to almost 50% of the global aridification expansion (Figure 6). Fu and Ma (2008) pointed out that the east of Northwest China and the North China experienced significant interdecadal transitional changes from wet to dry in the 1970s, and these two regions and the southeastern part of Northeast China exhibited significant trend of aridification. In addition, the frequency of extreme droughts in the eastern part of Northwest China, North China and Northeast China has increased significantly since the 1980s, with the largest increase being observed in Northeast China (Fu and Ma, 2008). Li et al. (2015) studied the aridification of northern China and also found that the expansion of the semi-arid regions in China mainly occurred in the middle and lower Yellow River, Heilongjiang Province and the Gansu Province.

3. Impact of marine activities on dryland climate changes

3.1 Impact of ocean oscillation factors and SST anomalies on temperature changes in drylands

In the context of long-term trends, the drylands show significant characteristics of interdecadal variations. Studies have shown that the interdecadal signals for the SST in different basins can cause atmospheric circulation anomalies, which affect the climate of different regions (Huang et al., 2017a), in particularly temperature changes. Changes in the SST causes stronger or weaker interdecadal signals of temperature (accelerating or slowing down global warming).

In the past 100 years, owing to the transformation of the positive and negative phases of the oscillation indexes, such as the Pacific Decadal Oscillation (PDO), the North Atlantic Oscillation (NAO), the Atlantic Multidecadal Oscillation (AMO), there have been two global warming slowing down periods in the world, the period from 1940 to 1975 and the period since the end of the 20th century (Kosaka and Xie, 2013; Huang et al., 2017b). Among these, the warming slowing down period at the end of the 20th century aroused widespread concerns. Huang et al. (2017b) have performed a lot of research on this phenomenon. The results indicated that the contribution from the land cooling to the NH was up to 66% in the cold season during the warming slowing down period, and the major cooling areas were located in Eurasia and North America which have large areas of drylands. Huang et al. (2017b) derived the decadal modulated oscillation (DMO) of the temperature and a long-term trend for temperature change using Ensemble Empirical Mode Decomposition (EEMD). As shown in Figure 7, the long-term trend of temperature change showed a continuously rising,

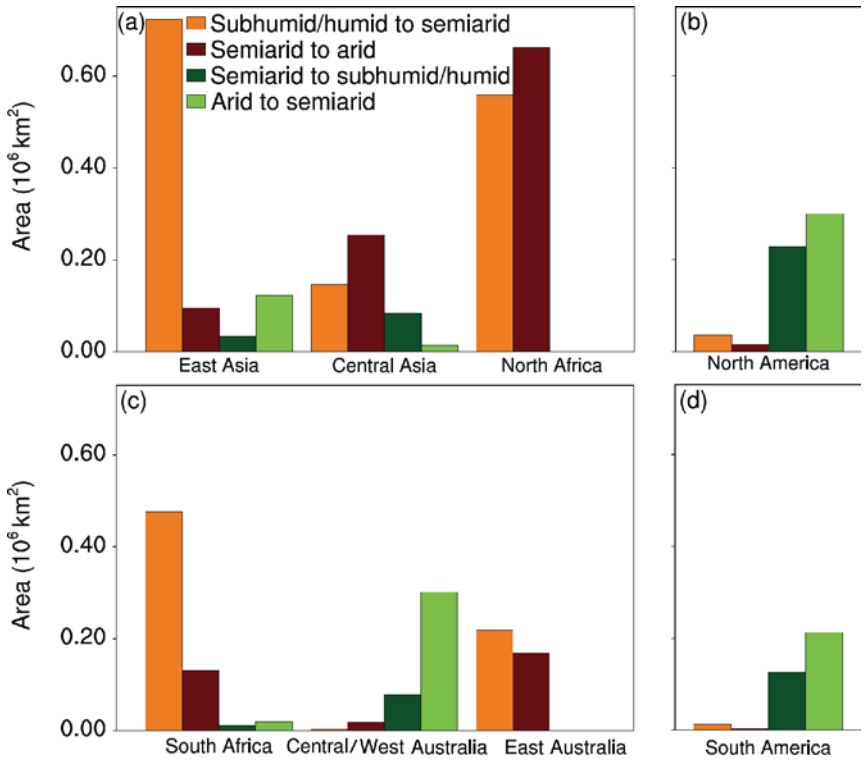

Figure 6 Area transitions of different climate zones over the eight semi-arid regions. (a) East Asia, Central Asia, northern Africa; (b) North America; (c) southern Africa, central/west Australia and east Australia; (d) South America. Cited from Huang et al. (2016). Orange represents the transition from a sub-humid/humid to a semi-arid region; brown represents the transition from a semi-arid to an arid region; dark green represents the transition from a semi-arid to a sub-humid/humid region; and light green represents the transition from an arid to a semi-arid region.

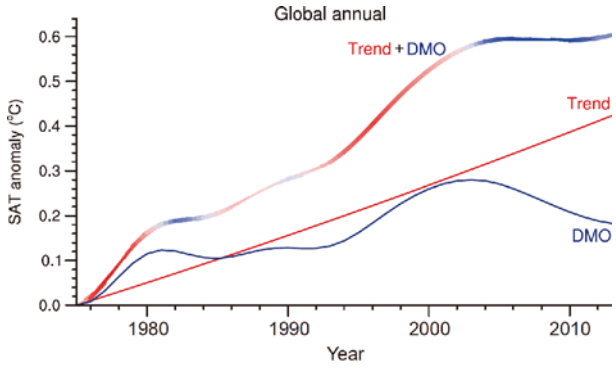

Figure 7 EEMD decomposed time series for long-term trends, DMO and their combination of the global mean temperature. Cited from Huang et al. (2017b).

while the DMO showed the changing characteristics of the oscillation. During the accelerated warming period, the DMO showed a rising trend. The overlapping of this rising DMO and long-term rising trend of the temperature resulted in rapid warming in the NH during this period. During the warming slowing down period, the DMO showed a downward trend, which offset the long-term temperature rise, and resulted in a warming slowdown across the world. Furthermore, Guan et al. (2015a) decomposed the original temperature change into the radiatively forced (RFT) and dynamically induced temperature changes (DIT) by using a dynamical adjustment method. As shown in Figure 8, the RFT refers to the temperature change caused by human factors, such as CO_2 emissions, and the DIT refers to the temperature change that is dominated by the internal variability of climate system. During the accelerated warming period, the DIT showed a rising trend. The overlap of the rising DIT and RFT caused accelerated warming during this period, while warming slowdown was caused by the cooling DIT which offset warming RFT. The cooling of DIT was caused by the joint action of the NAO, PDO and AMO. Studies by Guan et al. (2015a, 2015b) and Huang et al. (2017b) have shown that the interdecadal signals caused the transition between the accelerated warming and warming slowdown.

3.2 Impact of ocean oscillation factors and SST anomalies on the change of precipitation in drylands

Interdecadal signals, such as NAO, PDO, and AMO, cause atmospheric circulation anomalies, which in turn cause the slowing down of global warming, and furthermore affect the precipitation in drylands, resulting in dry and wet changes in different regions. After simulating the SST as a forced field, it was found that the ocean played an extremely important role in the climate change of semi-arid regions in the Sahel region. The severe drought in the Sahel region from the 1970s to the 1980s was mainly caused by warming of the

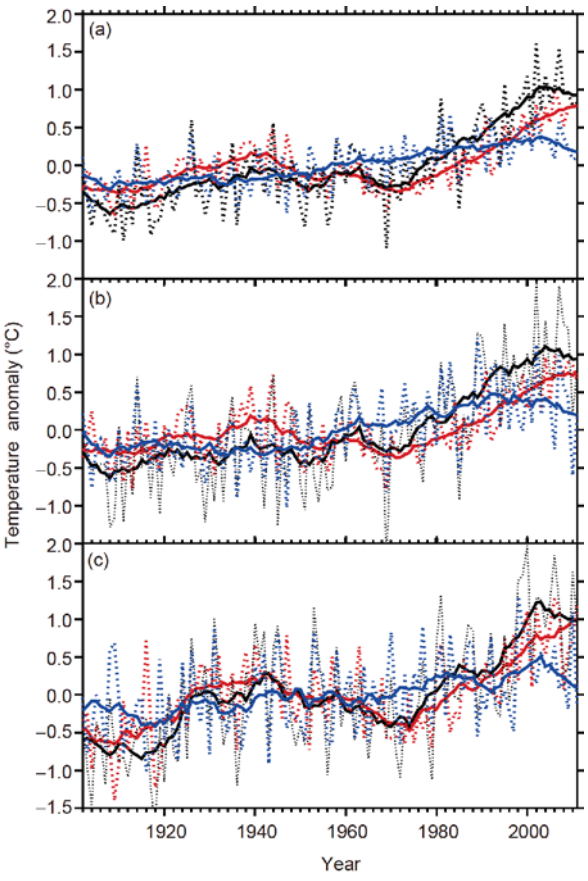

Figure 8 Regional mean time series for the raw temperature (black), DIT (blue) and RFT (red) over the (a) NH; (b) Eurasia; and (c) North America. Cited from Guan et al. (2015a).

tropical Atlantic Ocean and the Indian Ocean (Giannini et al., 2003, 2008; Bader and Latif, 2003; Lu and Delworth, 2005; Hoerling et al., 2006, 2010). Many studies concerning North America discovered that persistent SST anomalies in the Pacific Ocean and Atlantic Ocean strongly affected the precipitation in the United States by affecting the atmospheric circulation (Ting and Wang, 1997; Dai and Wigley, 2000; Schubert et al., 2009; Mo et al., 2009; Hu and Feng, 2012; Dai, 2013b; Dong and Dai, 2015). In particular, the Pacific Ocean played a key role in the precipitation in the drylands of the western United States. More than half of the interdecadal droughts in the United States were caused by the phase changes of the PDO and AMO (McCabe et al., 2004). In addition, climate change in the drylands of Asia were closely related to the PDO. In the semi-arid regions of northern China, drought tended to occur during the warm phase of the PDO (Ma and Fu, 2003, 2006; Ma and Shao, 2006; Ma, 2007; Qian and Zhou, 2014). Furthermore, the correlation coefficient calculated by Dai (2013b) between the original Niño3.4 index, the Niño3.4 index after high pass filtering, the Inter-decadal Pacific Oscillation (IPO) index and the global precipitation showed that the spatial distributions reflected by the three correlation maps on land

were basically the same and similar to the main mode of global land precipitation, indicating that El Niño Southern Oscillation (ENSO) (interannual) and PDO (interdecadal)) as the ocean oscillation factors are the main factors that affect the spatial distribution pattern of global land precipitation.

Previous experiments have proved that the model can easily reproduce the correlation between the precipitation changes and the PDO in global drylands (Schubert et al., 2009; Dong and Dai, 2015). Xu (2016) established a multiple linear regression equation of precipitation using the Niño3.4, PDO and AMO index, and selected five typical drylands for time fitting of the precipitation, as shown below:

$$\mathrm{Pre}(t) = b_0 + b_1 \times \mathrm{Niño3.4}(t) + b_2 \times \mathrm{AMO}(t) + b_3 \times \mathrm{PDO}(t).$$

Pre represents the fitted precipitation. The results showed that the precipitation in North Africa is more sensitive to the SST, and that the correlation coefficient of the time series between the fitted precipitation and the original precipitation was 0.66 (Figure 9). Meanwhile, the continuous decrease in the precipitation in North Africa during 1951–1985 was mainly due to the downward trend of the AMO and the rising trend of the PDO. The precipitation reduction caused by these two factors accounts for 57% of the change to the original precipitation. After 1985, the precipitation in North Africa changed to a rising trend, which is mainly due to the combination of the rising trend of the AMO and the downward trend of the PDO. Based on the coefficients of the multiple regression equation and the related statistics shown in Table 3, it was found that the long-term contribution of El Niño (b_1) to precipitation in North Africa was less than the contribution of AMO (b_2) and PDO (b_3). Therefore, the contribution of the AMO and PDO to the long-term trends of precipitation in North Africa have an equivalent magnitude, but opposite signs.

For North China, although the fitting curve of the precipitation passed the F test, only the regression coefficient of PDO (b_3 in Table 3) passed the significance test, and b_3 (PDO) is about five times that of b_1 (El Niño) and b_2 (AMO). During the time period of 1961–1985, precipitation in North China showed a decreasing trend, and a negative anomaly occurred in the precipitation at the end of the 1970s, which was mainly due to the downward trend of the PDO (Figure 9). With the transition of the PDO from a warm to a cold phase after the 1990s, the negative anomaly of precipitation in North China showed a weak upward trend. It should be pointed out here that although the aridification in North Africa (Nicholson et al., 1998, 2000) and North China has certain similarities (Huang, 2006a; Yan et al., 1990; Zhang and Chen, 1991; Huang et al., 1999), the SST signals which dominate them are significantly different. The precipitation in North Africa is affected by both the AMO and PDO, and the contributions from them are similar. The precipitation in North China is mainly dominated by the PDO, and the impact of the AMO is weak. In addition, the regression coefficients corresponding to the precipitation in the United States and North China have opposite signs, and the value for b_3 (PDO) is much larger than that for b_1 (El Niño) and b_2 (AMO), indicating that the precipitation in the United States is basically dominated by the PDO, followed by the AMO (Table 3). It was also proven that the precipitation in North China decreased while the precipitation in the United States increased when the PDO is in the warm phase, and vice versa (Ma, 2007; Dai, 2013b). McCabe et al. (2004) reported that the PDO and AMO contribute to more than 52% of the spatial and temporal variance of the interdecadal drought frequency in the United States. These results indicated that the precipitation in North China and the United States were mainly dominated by the PDO.

As there are significant regional differences in the response of precipitation from Australia to South America to SST anomalies, in discussions they are divided into the western and eastern parts. Compared to western Australia, the regressed precipitation in eastern Australia contributes more to the variance of the original precipitation, which is up to 46%. Meanwhile, the contribution of El Niño (b_1) to the variance of the precipitation in eastern and western Australia is much greater than that of the PDO and AMO (Table 3). In addition, the contribution of the fitted precipitation in the northern South America to the variance of the original precipitation mainly comes from El Niño (b_1) and PDO (b_3), while the contribution of the AMO (b_2) is relatively weak.

3.3 Impact of ocean oscillation factors and SST anomalies on the dry and wet changes in drylands

The global oceans are important forcing sources for the formation of global dry and wet distributions (Hua and Ma, 2009). At the same time, the drylands are sparsely precipitated and ecologically fragile, and are extremely sensitive to global ocean regulating factors. Numerous studies have shown that oceanic activities, especially SST anomalies in the Pacific and Atlantic basins, can significantly affect the dry and wet changes in drylands (Ting and Wang, 1997; Ting et al., 2011; Zhang and Delworth, 2006; Dai, 2013a; Trenberth and Hurrell, 1994; Trenberth et al., 2014). As the SST anomaly signals at the interannual and interdecadal scales of different basins can cause atmospheric circulation anomalies in the corresponding time scales, the characteristics of the dry and wet changes in drylands will be affected through teleconnections (Trenberth et al., 1998). These studies mainly reviewed the impact of the oceanic oscillation factors and the SST anomalies in the Pacific and Atlantic on the dry and wet changes in the drylands.

As the most significant interannual variation signal in the world, the ENSO signal can force the upper atmospheric

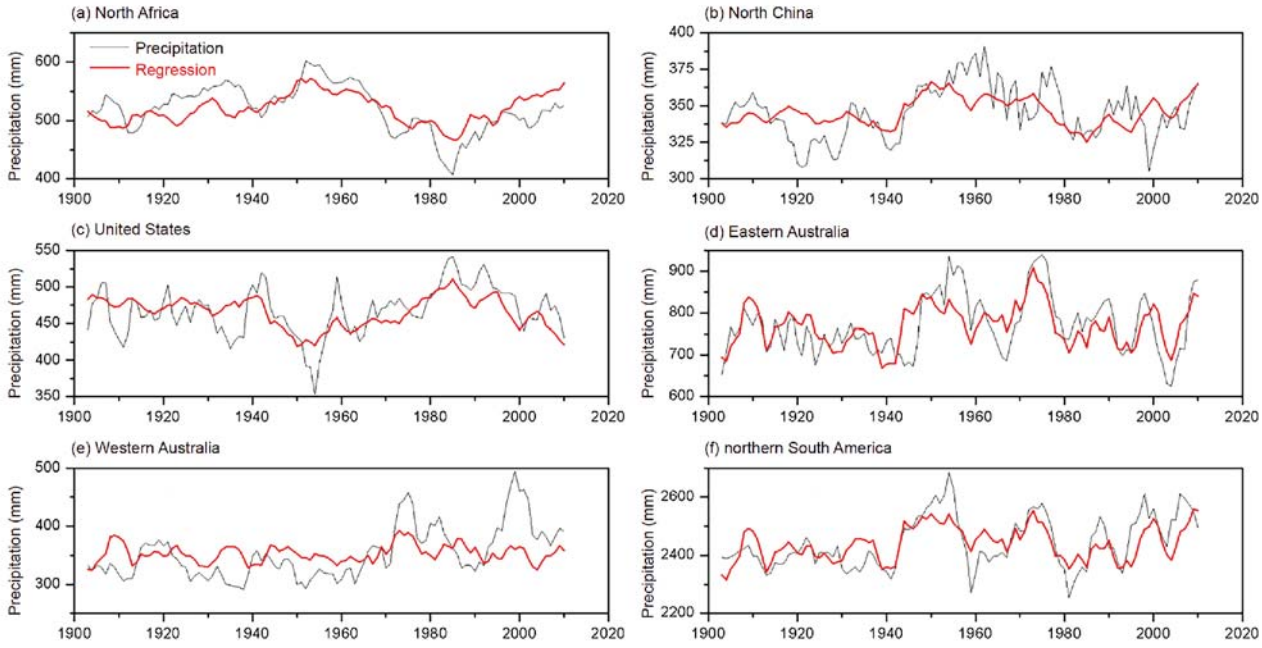

Figure 9 Time series for precipitation and fitted precipitation in typical regions of the world. Cited from Xu (2016).

Table 3 Coefficients of multiple regression equations (b_0, b_1, b_2, b_3) and the related statistics[a)]

	b_0	b_1	b_2	b_3	R^2	F	MSE
North Africa	520.3*	18.31*	22.55*	26.53*	0.44	28.04*	870.28
North China	346.0*	2.59	2.55	12.27*	0.27	13.37*	260.22
United States	464.8*	3.79	10.95*	24.89*	0.36	20.24*	832.96
Eastern Australia	770.5*	79.67*	18.13*	34.51*	0.46	30.73*	2924.14
Western Australia	352.2*	35.65*	9.21	5.09	0.11	4.58*	1779.95
northern South America	2439.7*	92.90*	9.83	39.87*	0.44	28.43*	4560.01
southern South America	1432.9*	2.74	1.76	9.79	0.01	0.27	6382.14

a) * indicates that the regression coefficient and the equation pass the significant test of α=0.05. R^2 represents the square of the correlation coefficient, and F indicated whether the regression equation is significant. MSE represents the root mean square error. Cited from Xu (2016).

circulation, activate and maintain atmospheric circulation anomalies, and further trigger global dry and wet changes. El Niño, which occurs in the equatorial Pacific, is the most critical contributor to tropical drought (Hoerling and Kumar, 2003; Coelho and Goddard, 2009; Trenberth et al., 2014). Under the influence of a strong El Niño oscillation, the global dry land range is twice that compared to a weak El Niño (Lyon, 2004). In different regions and seasons, impact of ENSO on wet and dry changes in the global drylands also shows some differences (Ropelewski and Halpert, 1987; Dai and Wigley, 2000). A study found that, when El Niño occurred, drought usually occurred in South Africa, as it was rainy from the end of the year to the beginning of the next year in the drylands of East Africa. In East Asia, owing to the increase in the SST in the eastern equatorial Pacific and enhancement of the Hadley Cell, the Pacific subtropical high was enhanced, and the position extended southward, meaning that the summer monsoon was weak, the northward strength of the warm and humid airflow was weak, and the cold air moved to the South. Therefore, the monsoon rain zone generated by the convergence of cold and warm air stagnates in the middle and lower Yangtze River, causing continuous rain and floods for East Asia in the summer (Huang, 2006b). PDO is an oscillated-type of SST similar to El Niño that occurs in the North Central Pacific (Mantua et al., 1997; Mantua and Hare, 2002), and lasts between 20 and 30 years, and is also known as the "decadal El Niño phenomenon". The PDO is generally considered to be a part of IPO in the North Pacific. As interdecadal signals in the Pacific Oceans, they both affect the dry and wet changes in the drylands. Previous results showed that the continuous drought in the north China region from the mid-to-late 1970s was closely related to the change in the PDO from the cold to the warm phase in 1976 (Ma and Shao, 2006; Ma, 2007). The cold and warm phases of the IPO correspond to a reduction and increase in the precipitation in the central and western

parts of the United States (Dai, 2013b), respectively.

The impact of the Atlantic SST anomalies on global dry and wet climate changes cannot be ignored (Sutton and Hodson, 2005; Knight et al., 2006; Zhang and Delworth, 2006). SST anomalies in the equatorial Pacific and Atlantic both affect the precipitation in southeastern South America, but the time scales of impact are different. Among these, the equatorial Pacific mainly acts on the interannual time scale, while the equatorial Atlantic acts on the interdecadal time scale or longer. Corresponding to the cold phase of the AMO in the 20th century, the southeastern part of South America became continuously wet (Seager et al., 2010). Ting et al. (2011) reported that, when the AMO was in the warm phase, the Atlantic equatorial convergence zone moved northward, resulting in increased precipitation in western Sahel in Africa, the equatorial north Atlantic, and the central United States, while the precipitation decreased in western South Africa, the equatorial south Atlantic, and eastern South America. Yang et al. (2017) reported that, when the AMO is in the positive phase, most regions in the eastern hemisphere experience more precipitation, except for Central America and northern South America, as the precipitation in the western hemisphere is reduced. When AMO is in the negative phase, the precipitation in the eastern hemisphere is reduced and the precipitation in the western hemisphere is increased. Compared with the PDO, the degree of precipitation anomalies in the global land areas caused by AMO is relatively small, and the high-impact areas are mainly concentrated in Africa and northern South America.

Huang et al. (2016) showed that the global drylands have been expanding over the past 60 years due to global warming. Dai et al. (2004) discovered that the global very dry areas have increased by more than twice since the 1970s, and global very wet areas have decreased, which is mainly related to the decrease of the precipitation and global warming caused by ENSO in the 1980s. However, in the latest research by Guan et al. (2017), it was reported that the long-term drought in the middle and high latitudes of the NH was alleviated during the warming slowdown period, mainly including the drylands in Eurasia and North America. This change was mainly measured using the AI. During the warming slowdown period, the temperature was still at a high level, and a change in the evaporation was not significant. However, the atmospheric circulation anomaly caused by the phase transition of the interdecadal index led to an increase in precipitation, and the AI also increased, as shown in Figure 10. Guan et al. (2017) further decomposed the AI into the dynamically induced AI (DAI) and the radiatively forced AI (RAI) using the dynamical adjustment method. The analysis found that the reversal of the AI is dominated by the slowdown of the decline of the DAI, and the slowdown of the DAI decline is also closely related to the phase changes of NAO, PDO and AMO. At the same time,

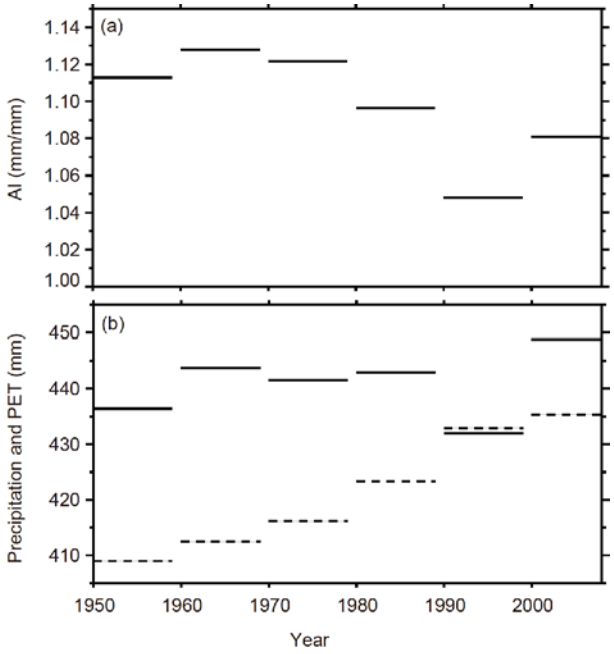

Figure 10 Decadal variability for different variables: (a) AI; and (b) P (solid line) and PET (dashed line). Cited from Guan et al. (2017).

Guan et al. (2017) also reported that, although the long-term drought in the middle and high latitudes of the NH was alleviated during the warming slowdown period, this was only temporary. Once the phase of the NAO, PDO and AMO changed, the world will change to a period of accelerated warming, and the existing slowdown period of drying will also disappear.

4. Mechanism of impact of the ocean oscillation factors on dryland climate changes

Compared to atmospheric motion, the movement and change of the oceans is slower and obviously more persistent. Abnormal signals of atmospheric circulation can be stored in oceans through the interaction of oceans and the atmosphere, and these abnormal signals are then transferred to the atmosphere, causing abnormal circulation, which in turn affects climate change in drylands (Wu et al., 2007, 2008). The SST anomalies play an important role in the variation of interdecadal precipitation. The SST anomalies in different basin regions around the world induces the variations of land-sea thermal contrasts and north-south thermal contrasts, thus affecting the westerly jet, planetary waves, blocking frequencies and Asian monsoons (Huang et al., 2017a). At the same time, the interaction between the anomalous atmospheric circulation and the SST anomalies will further affect climatic factors such as the regional precipitation and temperature (Huang et al., 2010; Hu et al., 2018). For example, the warm phase of the ENSO-like model plays an

important role in the increase of the spring precipitation in southeastern China and the reduction of precipitation in northern China (Yang and Lau, 2004). The tropical SST anomaly in the second half of the 20th century dominated the decadal weakening trend of the Asian summer monsoon. When the El Niño occurred, a large range of abnormal seawater warming occurred in the equatorial central and eastern Pacific, and traditional southeast trade winds and equatorial ocean currents were greatly weakened, resulting in changes in the global atmospheric circulation. Among these, the most direct phenomenon is the "seesaw" phenomenon of the reversed-pressure anomaly between the Southeast Pacific and the Indian Ocean, as well as Indonesia. When the air pressure in the Southeast Pacific becomes high (low), the air pressure in the Indian Ocean and Indonesia becomes low (high), this is the Southern Oscillation (SO) phenomena (Halpert and Ropelewski, 1992). This anomaly of air pressure leads directly to a decrease in the pressure gradient between the eastern and western Pacific, weakening the southeast trade winds, the equatorial ocean currents and the Walker circulation, and ascending branch of the Walker circulation moved eastward, thus affecting climate change in the drylands of Australia.

During the summer of El Niño's retreat year, the SST anomaly in the Indian Ocean can store El Niño's warm signal until the summer through the "capacitor effect", inducing Kelvin waves in the atmosphere, causing an anticyclonic anomaly in the Pacific Northwest, thus affecting the East Asian summer monsoon (Xie et al., 2009, 2016). Nitta (1986, 1987) and Huang et al. (2004) found that the convective activity in the tropical northwestern Pacific has an oscillating relationship with the summer precipitation in East Asia. Therefore, the ENSO signal can also excite the teleconnection pattern in summer through the "capacitor" of the Indian Ocean, thus affecting the summer precipitation in the drylands in northwest China, especially in the marginal regions of the monsoon, by affecting the monsoon swing (Huang and Wu, 1989; Huang and Sun, 1992). In addition, the local air-sea feedback mechanism of the Northwest Pacific can also maintain the El Niño signal until early summer (Wang et al., 2000). These two mechanisms are not contradictory. The local feedback mechanism in the northwest Pacific exists in spring and causes warming of the North Indian Ocean. In the summer, the warming of the North Indian Ocean further stimulates the teleconnection anomaly, that is, the local feedback process in the tropical northwest Pacific and the capacitor mechanism of the Indian Ocean are interconnected and undergo mutual feedback, which is known as the Indo-western Pacific Ocean capacitor (IPOC) effect (Kosaka and Nakamura, 2006, 2010; Kosaka et al., 2009, 2011).

Furthermore, during the El Niño, the anomalous warming of the SST in the equatorial central and eastern Pacific led to an enhanced local convective activity, combined with the teleconnection effect, which caused the anomalous circulation in the middle and high latitude regions of the NH and excited the Pacific/North American (PNA) (Horel and Wallace, 1981; Shukla and Wallace, 1983; Wu and Chen, 1992; Straus and Shukla, 2002). El Niño excites a positive PNA circulation pattern, while La Niña tends to correspond to a negative PNA pattern, which affects the climate in North America, especially in the drylands of Western North America. When PNA is in the positive phase, the temperature in the drylands of Western North America is significantly higher under the influence of strong pressure ridges, and the impact on precipitation is not obvious, but the probability of reduced precipitation is greater. Conversely, when the La Niña occurs, the temperature in the drylands of Western North America is lower, and the probability of more precipitation is slightly higher.

There is also a relationship between the ENSO and NAO (Huang et al., 1998). As early as 1984, Rogers reported that a relationship between NAO and SO could be established through Rossby waves on the quasi-six-year time scale. Huang et al. (1998) further discovered that the relationship between NAO and ENSO on the quasi-six-year time scale is not stable. There was a good relationship between the two in 1910–1960, and this relationship then gradually weakened or even disappeared. During a strong El Niño event, the heat source anomalies in the equatorial central and eastern Pacific excite the PNA pattern in the mid-high latitudes of the NH through teleconnections, and also excite a positive NAO pattern circulation anomaly in the Atlantic region, that is, NAO is well correlated with ENSO, which in turn affects the climate in Europe and the surrounding areas of the Mediterranean, including the drylands of North Africa. When a weak El Niño event occurs, the correlation between the NAO and ENSO is weak.

Ding et al. (2009) also reported that the SST in the central and eastern tropical Pacific is positively correlated with the precipitation in the Yangtze River Basin and most areas of South China, and negatively correlated with the precipitation in North China. As the main pattern in the Pacific, the PDO and IPO have significant effects on the regional precipitation (Trenberth and Hurrell, 1994; Dai, 2013a; Ma, 2007; Duan et al., 2013). The positive and negative phases of the PDO also have a significant impact on the precipitation in drylands. When the PDO is in a positive phase, the warm SST anomaly in the equatorial Middle East Pacific increases the sensible heat flux from the ocean to the atmosphere, heating the entire tropical troposphere, and causing a positive temperature anomaly (Figure 11a). At the same time, the tropospheric temperature in the mid-latitudes of the NH will be abnormally low, thus changing the meridional temperature gradients in the North Pacific and the surrounding areas. Thus, the meridional temperature gradient in the subtropical to the mid-latitude (15°N–45°N) increases. According to the prin-

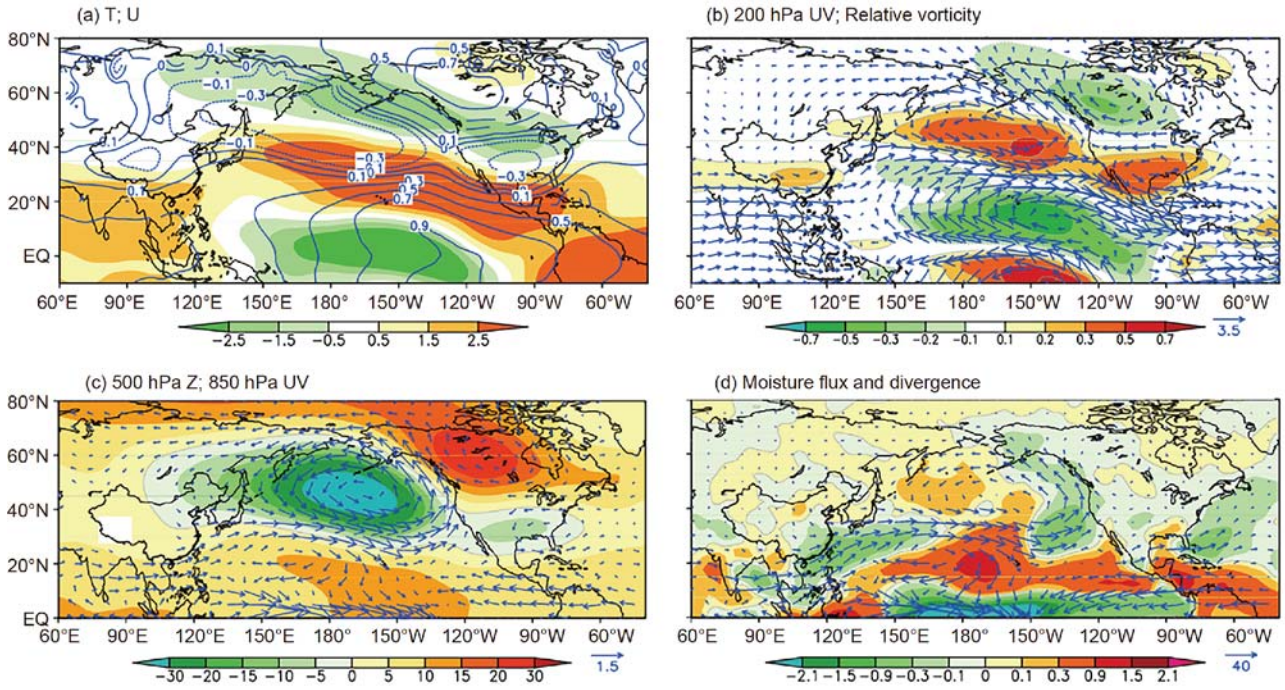

Figure 11 Response of the atmospheric circulation to the positive phase of PDO. (a) Tropospheric temperature (200 hPa, K, contour) and 200 hPa zonal wind (m s^{-1}, shading); (b) 200 hPa wind field (m s^{-1}, vector) and relative vorticity (1×10^5, s^{-1}, shading); (c) 500 hPa geopotential height (m, shading) and 850 hPa wind field (m s^{-1}, vector); and (d) column-integrated moisture flux (g cm^{-1} s^{-1}, vector) and moisture divergence (mm day^{-1}, shading). Cited from Yang et al. (2017).

ciple of thermal wind, the westerly wind in the area is enhanced; while the meridional temperature gradient in the tropics and the high latitudes weaken, this correspondingly leads to an abnormal eastern wind. This wind field anomaly causes a vorticity shear of "negative in the south and positive in the north" in the upper layer of the North Pacific troposphere, that is, anomalous cyclones in the northern North Pacific and anomalous anticyclones in the southern North Pacific (Figure 11b). As a result, the Aleutian Low is enhanced and the subtropical high is also enhanced (Figure 11c). At the corresponding bottom layer of the troposphere, a large range of cyclonic wind fields appear in the northern North Pacific, and an anticyclonic wind field appears in the Northwest Pacific. An abnormal southwesterly wind appears in the south of the Yangtze River and an abnormal northwesterly wind appears in North China. This abnormal wind field will weaken the East Asian summer monsoon and prevent the northward movement of tropical water vapor and rain belts (Figure 11d), which will reduce the precipitation in North China, while the precipitation is more concentrated in the south of the Yangtze River, and eastern China will experience a pattern of "southern flooding and northern drought". Huang et al. (2016) also reported that the drying trend in the eastern hemisphere is related to the weakening of the East Asian summer monsoon. When the PDO is in a negative phase, the response of the atmospheric circulation is reversed, and eastern China will experience a pattern of "southern drought and northern flooding".

In addition, owing to the multi-decadal variation of the Atlantic SST, the AMO affects the interdecadal variations of precipitation in eastern China through modulation of the PDO by the teleconnection wave train (Si and Ding, 2016). Zhu et al. (2016) indicated that when the PDO is in the warm phase and the AMO is in the cold phase, the precipitation in the lower reaches of the Yangtze River is a positive anomaly, and vice versa. Using a numerical model to simulate the impact of the interdecadal SST on climate change, Yang et al. (2017) discovered that when the PDO was in the neutral mode and the AMO was in the warm phase (Figure 12a), an eastward propagating wave train was excited and an abnormally high pressure was found in the North Pacific, that is, the Aleutian Low was weakened and the corresponding subtropical high was also weakened. Anticyclonic anomalies occurred in the lower troposphere in the northern Pacific, resulting in anomalous southwesterly winds in North China and anomalous easterly winds in the south of the Yangtze River. This anomalous wind field will strengthen the East Asian monsoon, and eastern China will experience a pattern of southern drought and northern flooding, and vice versa. In contrast, the intensity of the abnormal high pressure induced by the AMO warm phase (Figure 12a) is approximately half of the abnormal high-pressure intensity induced by the PDO in the cold phase (Yang et al., 2017), indicating that the atmospheric circulation shows an opposite response to the same phases of AMO and PDO, but the response of the atmospheric circulation to the AMO is weaker, which is

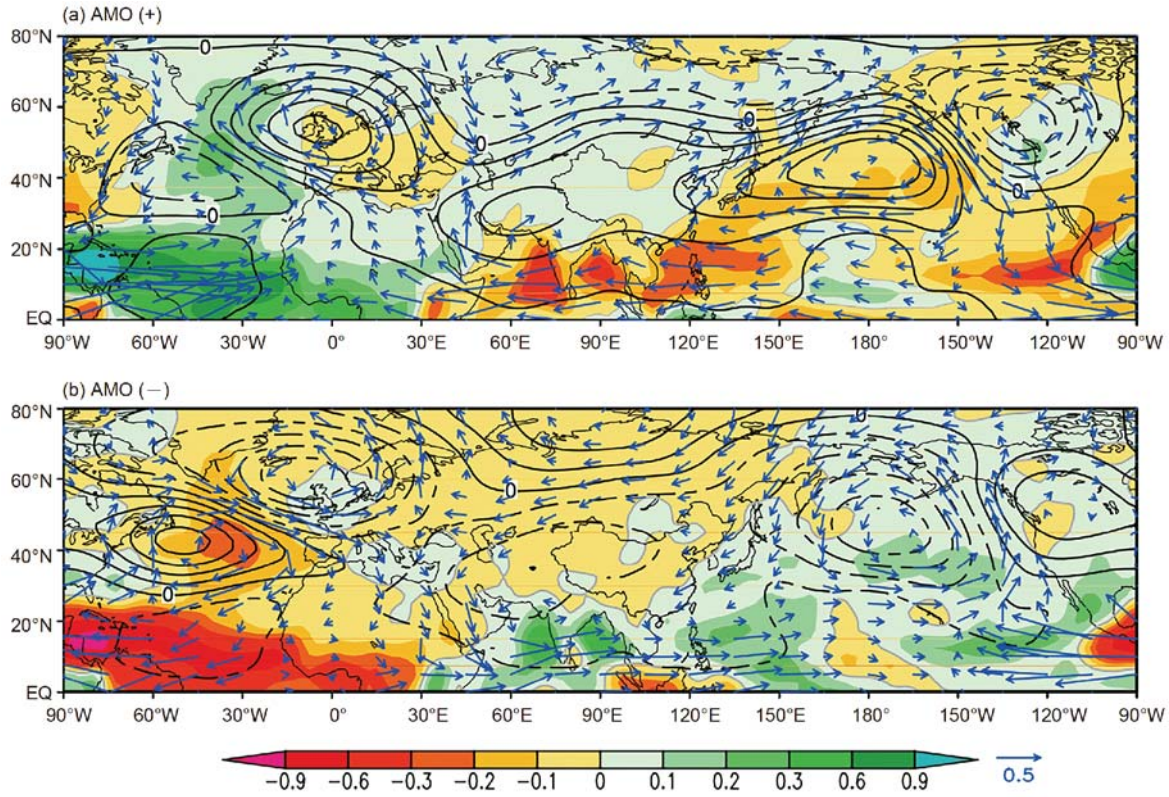

Figure 12 Response of the atmospheric circulation to the AMO: (a) positive phase; and (b) negative phase. Precipitation (mm day^{-1}, shading), 500 hPa geopotential height (shading) and 850 hPa wind field (m s^{-1}, vector). Cited from Yang et al. (2017).

consistent with the results reported by Zhu et al. (2016). In addition, Si and Ding (2016) reported that the AMO warm (cold) phase will cause a warm (cold) SST anomaly in the mid-latitude West Pacific and central Pacific, inducing a positive (negative) anomaly for the geopotential height field in the Yellow River Basin and a negative (positive) anomaly for the height field in the Yangtze River Basin through a stationary baroclinic wave train in the NH, that is the teleconnection wave train from the North Atlantic to Eurasia and extending to North America. Eventually, these anomalous atmospheric circulation fields cause positive (negative) precipitation anomalies in North China and negative (positive) precipitation anomalies in South China. The numerical simulation results shown in Figure 13a indicate that when the AMO is in a neutral mode, the precipitation in the south of the Yangtze River decreases by 0.24 mm day^{-1} in the PDO cold phase, and the precipitation in the south of the Yangtze River increases by 0.31 mm day^{-1} in the PDO warm phase. Conversely, when the PDO is in a neutral condition, the precipitation in the south of the Yangtze River decreases by 0.04 mm day^{-1} in the AMO warm phase, but the precipitation in the south of the Yangtze River increases by 0.07 mm day^{-1} in the AMO cold phase. Therefore, the response intensity of the precipitation in the south of the Yangtze River to the AMO warm (cold) phase is about one fifth of the contribution of the PDO cold (warm) phase. This indicates that in terms of precipitation, there is an opposite response to the AMO and the PDO, suggesting that the PDO dominates the change in the precipitation in the south of the Yangtze River, and the contribution of the AMO is relatively small. In addition, the combination of the different phases of the AMO and the PDO will affect the distribution pattern of the interdecadal precipitation in eastern China (Figure 13). When the PDO is in the warm phase, "southern drought and the northern flooding" pattern will form. At this time, if the AMO and PDO are in opposite phases, this pattern will be strengthened, and if the AMO and PDO are in the same phase, this pattern will be weakened (Yang et al., 2017).

5. Conclusion

In summary, the effect of climate change in drylands on global changes cannot be ignored. Under the backdrop of global warming, the total area of drylands has expanded significantly, and extreme drought events have occurred frequently. During the process of climate change in the past 100 years, the semi-arid regions have shown significant periods of enhanced warming and aridification, and there has been prominent spatial differences, resulting in the deterioration of the local environment. As a major component of the Earth's climate system, the impact of the oceans on cli-

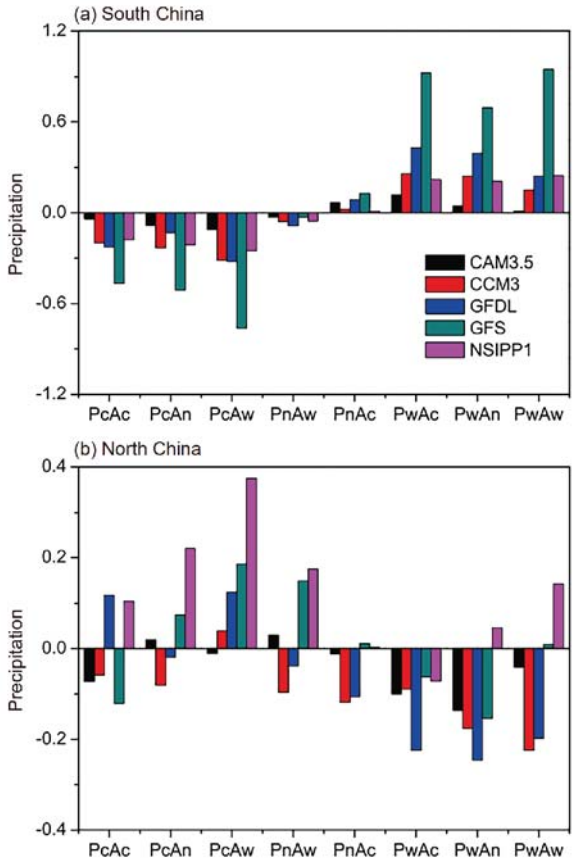

Figure 13 Difference in average annual precipitation over (a) South China and (b) North China in eight experiments from that of the control experiment (PnAn) for all five participating AGCMs. Pc/Pw represents the positive cold/warm anomaly of PDO; Ac/Aw represents the cold/warm anomaly of AMO; Pn/An represents the neutral anomaly of PDO and AMO. Cited from Yang et al. (2017).

mate change in drylands is mainly reflected in the variation characteristics of temperature, precipitation, and dry and wet changes on the interdecadal scale. The SST anomalies in different sea basins can significantly affect climate change in drylands. The oceanic oscillation factors cause the interdecadal modulation of oscillations to display upwards or downwards trends through different phase transitions, which overlaps on the long-term upward trends of temperature, thus causing the temperature in drylands to shows interdecadal variation characteristics of accelerated warming or warming slowdown. At the same time, the oceanic oscillation factors such as ENSO, PDO, AMO and NAO change the land-sea thermal contrasts through different phase transitions, causing atmospheric circulation anomalies and global temperature changes, which in turn affects the precipitation and dry/wet changes in drylands.

Aiming to understand the impact of oceans on climate change in drylands, a large number of studies have been carried out, and a series of progress has been achieved, but there is a lack of comparative studies on the interdecadal variations of temperature, precipitation, and dry and wet changes at different scales around the world. Our understanding of the relevance and differences among the different regions is still not sufficient. In addition, there are relatively few studies on how the interaction of different sea areas affects climate change in drylands. At present, it is still impossible to quantitatively distinguish the relative contributions of different ocean oscillation factors in the climate evolution of drylands and their response processes. Meanwhile, our understanding of the climate evolution mechanisms of drylands affected by air-sea interactions is not sufficient. In the future, a comprehensive and systematic study on these mechanisms should be carried out by combining various observational data sources and numerical simulations. Climate warming and increasing aridity will increase the risk of desertification, and there are also significant uncertainties about the future in terms of climate change in drylands. Therefore, it is necessary to further investigate the impact of oceans on climate change and the ecological environment in drylands, and to deepen our understanding of the climate evolution mechanisms in drylands, so as to provide a reliable scientific basis for predicting future climate change in drylands and prevent desertification.

Acknowledgements *We thank to the anonymous reviewers for their valuable comments and constructive suggestions. This work was supported by the National Natural Science Foundation of China (Grant Nos. 41722502, 41521004, 41575006 & 91637312) and the China Overseas Expertise Introduction Project for Discipline Innovation (111 Project) (Grant No. B13045).*

References

Armah F A, Odoi J O, Yengoh G T, Obiri S, Yawson D O, Afrifa E K A. 2010. Food security and climate change in drought-sensitive savanna zones of Ghana. Mitig Adapt Strateg Glob Change, 16: 291–306
Ault T R, George S S. 2010. The magnitude of decadal and multidecadal variability in North American precipitation. J Clim, 23: 842–850
Bader J, Latif M. 2003. The impact of decadal-scale Indian ocean sea surface temperature anomalies on Sahelian rainfall and the North Atlantic oscillation. Geophys Res Lett, 30: 2169
Bichet A, Wild M, Folini D, Schär C. 2011. Global precipitation response to changing forcings since 1870. Atmos Chem Phys, 11: 9961–9970
Cai W J, Cowan T, Thatcher M. 2012. Rainfall reductions over Southern Hemisphere semi-arid regions: The role of subtropical dry zone expansion. Sci Rep, 2: 702
Coelho C A S, Goddard L. 2009. El Niño-induced tropical droughts in climate change projections. J Clim, 22: 6456–6476
Dai A G. 2011a. Drought under global warming: A review. Wires Clim Change, 2: 45–65
Dai A G. 2011b. Characteristics and trends in various forms of the Palmer drought severity index during 1900–2008. J Geophys Res, 116: D12115
Dai A G. 2013a. Increasing drought under global warming in observations and models. Nat Clim Change, 3: 52–58
Dai A G. 2013b. The influence of the inter-decadal Pacific oscillation on US precipitation during 1923–2010. Clim Dyn, 41: 633–646
Dai A G, Trenberth K E, Qian T. 2004. A global dataset of Palmer drought severity index for 1870–2002: Relationship with soil moisture and effects of surface warming. J Hydrometeorol, 5: 1117–1130
Dai A G, Wigley T M L. 2000. Global patterns of ENSO-induced pre-

cipitation. Geophys Res Lett, 27: 1283–1286
Delworth T, Manaba S. 1993. Climate variability and land-surface processes. Adv Water Resour, 16: 3–20
Ding Y, Sun Y, Wang Z, Zhu Y, Song Y. 2009. Inter-decadal variation of the summer precipitation in China and its association with decreasing Asian summer monsoon Part II: Possible causes. Int J Climatol, 29: 1926–1944
Dong B, Dai A G. 2015. The influence of the interdecadal Pacific oscillation on temperature and precipitation over the globe. Clim Dyn, 45: 2667–2681
Duan W, Song L, Li Y, Mao J. 2013. Modulation of PDO on the predictability of the interannual variability of early summer rainfall over south China. J Geophys Res-Atmos, 118: 13008–13021
Dai A G, Zhao T B. 2017. Uncertainties in historical changes and future projections of drought, Part I: Estimates of historical drought changes. Clim Change, 144: 519–533
Feng S, Fu Q. 2013. Expansion of global drylands under a warming climate. Atmos Chem Phys, 13: 10081–10094
Fu C B, Huang Y. 1996. Global change in Asia (in Chinese). Clim Environm Res, 1: 97–112
Fu C B, Jiang Z H, Guan Z Y, He J H, Xu Z F. 2008. Climate of China and East Asian Monsoon. Berlin: Springer-Verlag. 1–48
Fu C B, Ma Z G. 2008. Global change and regional aridification (in Chinese). Chin J Atmosp Sci, 32: 752–760
Fu C B, Mao H T. 2017. Aridity Trend in Northern China. Singapore: World Scientific
GLP. 2005. Global Land Project: Science Plan and Implementation Strategy. IGBP (International Geosphere Biosphere Program) Report No. 53. In: International Human Dimensions Programme Report No. 19. Stockholm: IGBP Secretariat
Giannini A, Saravanan R, Chang P. 2003. Oceanic forcing of Sahel rainfall on interannual to interdecadal time scales. Science, 302: 1027–1030
Giannini A, Biasutti M, Verstraete M M. 2008. A climate model-based review of drought in the Sahel: Desertification, the re-greening and climate change. Glob Planet Change, 64: 119–128
Greve P, Orlowsky B, Mueller B, Sheffield J, Reichstein M, Seneviratne S I. 2014. Global assessment of trends in wetting and drying over land. Nat Geosci, 7: 716–721
Gu G J, Adler R F. 2013. Interdecadal variability/long-term changes in global precipitation patterns during the past three decades: Global warming and/or pacific decadal variability? Clim Dyn, 40: 3009–3022
Gu G, Adler R F. 2015. Spatial patterns of global precipitation change and variability during 1901–2010. J Clim, 28: 4431–4453
Guan X D, Huang J P, Guo R X, Yu H P, Lin P, Zhang Y T. 2015a. The role of dynamically induced variability in the recent warming trend slowdown over the Northern Hemisphere. Sci Rep, 5: 12669
Guan X D, Huang J P, Guo R X, Yu H, Lin P, Zhang Y. 2015b. Role of radiatively forced temperature changes in enhanced semi-arid warming in the cold season over east Asia. Atmos Chem Phys, 15: 13777–13786
Guan X D, Huang J P, Guo R X. 2017. Changes in aridity in response to the global warming hiatus. J Meteorol Res, 31: 117–125
Hulme M. 1996. Recent climatic change in the world's drylands. Geophys Res Lett, 23: 61–64
Halpert M S, Ropelewski C F. 1992. Surface-temperature patterns associated with the southern oscillation. J Clim, 5: 577–593
Hoerling M, Eischeid J, Perlwitz J. 2010. Regional precipitation trends: Distinguishing natural variability from anthropogenic forcing. J Clim, 23: 2131–2145
Hoerling M, Hurrell J, Eischeid J, Phillips A. 2006. Detection and attribution of twentieth-century northern and southern African rainfall change. J Clim, 19: 3989–4008
Hoerling M, Kumar A. 2003. The perfect ocean for drought. Science, 299: 691–694
Horel J D, Wallace J M. 1981. Planetary-scale atmospheric phenomena associated with the Southern Oscillation. Mon Weather Rev, 109: 813–829
Hu K M, Huang G, Wu R G, Wang L. 2018. Structure and dynamics of a wave train along the wintertime Asian jet and its impact on East Asian climate. Clim Dyn, 51: 4123–4137
Hu Q, Feng S. 2012. AMO- and ENSO-driven summertime circulation and precipitation variations in North America. J Clim, 25: 6477–6495
Hua L J, Ma Z G. 2009. The evolution of dry and wet periods in Asia and North America and its relationship with SSTA (in Chinese). Chin J Geophys, 52: 1184–1196
Huang G. 2006a. Global climate change phenomenon associated with the droughts in North China (in Chinese). Clim Environ Res, 11: 28–37
Huang G, Hu K, Xie S P. 2010. Strengthening of tropical Indian Ocean teleconnection to the Northwest Pacific since the Mid-1970s: An atmospheric GCM study. J Clim, 23: 5294–5304
Huang G, Liu Y, Huang R. 2011. The interannual variability of summer rainfall in the arid and semiarid regions of Northern China and its association with the northern hemisphere circumglobal teleconnection. Adv Atmos Sci, 28: 257–268
Huang J P, Guan X D, Ji F. 2012. Enhanced cold-season warming in semi-arid regions. Atmos Chem Phys, 12: 5391–5398
Huang J P, Ji M X, Xie Y K, Wang S S, He Y L, Ran J J. 2016. Global semi-arid climate change over last 60 years. Clim Dyn, 46: 1131–1150
Huang J P, Li Y, Fu C B, Chen F H, Fu Q, Dai A, Shinoda M, Ma Z, Guo W, Li Z, Zhang L, Liu Y, Yu H, He Y, Xie Y, Guan X, Ji M, Lin L, Wang S, Yan H, Wang G. 2017a. Dryland climate change: Recent progress and challenges. Rev Geophys, 55: 719–778
Huang J P, Xie Y K, Guan X D, Li D D, Ji F. 2017b. The dynamics of the warming hiatus over the Northern Hemisphere. Clim Dyn, 48: 429–446
Huang J P, Yu H P, Dai A, Wei Y, Kang L T. 2017c. Drylands face potential threat under 2°C global warming target. Nat Clim Change, 7: 417–422
Huang J P, Higuchi K, Shabbar A. 1998. The relationship between the North Atlantic oscillation and El Niño-Southern oscillation. Geophys Res Lett, 25: 2707–2710
Huang R H. 2006b. Progresses in research on the formation mechanism and prediction theory of severe climatic disasters in China (in Chinese). Adv Earth Sci, 21: 565–575
Huang R H, Sun F. 1992. Impacts of the tropical western Pacific on the East Asian Summer Monsoon. J Meteorol Soc Jpn, 70: 243–256
Huang R H, Wu Y F. 1989. The influence of ENSO on the summer climate change in China and its mechanism. Adv Atmos Sci, 6: 21–32
Huang R H, Chen W, Yang B L, Renhe Z. 2004. Recent advances in studies of the interaction between the East Asian winter and summer monsoons and ENSO cycle. Adv Atmos Sci, 21: 407–424
Huang R H, Wei Z G, Li S S, Zhou L T. 2006. The interdecadal variations of climate and hydrology in the upper reach and source area of the yellow river and their impact on water resources in North China (in Chinese). Clim Environ Res, 11: 245–258
Huang R H, Xu Y H, Zhou L T. 1999. The interdecadal variation of summer precipitations in China and the drought trend in North China (in Chinese). Plateau Meteorol, 18: 465–476
IPCC. 2007. Climate Change. The Physical Science Basis. Contribution of Working Group I to the Fourth Assessment Report of the Intergovernmental Panel on Climate Change
IPCC. 2013. Climate Change. The Physical Science Basis. Contribution of Working Group I to the Fourth Assessment Report of the Intergovernmental Panel on Climate Change
Knight J R, Folland C K, Scaife A A. 2006. Climate impacts of the Atlantic multidecadal oscillation. Geophys Res Lett, 33: L17706
Kosaka Y, Nakamura H. 2006. Structure and dynamics of the summertime Pacific-Japan teleconnection pattern. Q J R Meteorol Soc, 132: 2009–2030
Kosaka Y, Nakamura H, Watanabe M, Kimoto M. 2009. Analysis on the dynamics of a wave-like teleconnection pattern along the summertime Asian jet based on a reanalysis dataset and climate model simulations. J Meteorol Soc Jpn, 87: 561–580
Kosaka Y, Nakamura H. 2010. Mechanisms of meridional teleconnection observed between a summer monsoon system and a subtropical anticyclone. Part I: The Pacific-Japan pattern. J Clim, 23: 5085–5108
Kosaka Y, Xie S P, Nakamura H. 2011. Dynamics of interannual variability

in summer precipitation over East Asia. J Clim, 24: 5435–5453
Kosaka Y, Xie S P. 2013. Recent global-warming hiatus tied to equatorial Pacific surface cooling. Nature, 501: 403–407
Lambert F H, Allen M R. 2009. Are Changes in global precipitation constrained by the tropospheric energy budget? J Clim, 22: 499–517
Li C Y, Zhu J H, Sun Z B. 2002. The study interdecadal climate variation (in Chinese). Clim Environ Res, 7: 209–219
Li J W, Liu Z F, He C, Tu W, Sun Z X. 2016. Are the drylands in northern china sustainable? A perspective from ecological footprint dynamics from 1990 to 2010. Sci Total Environ, 553: 223–231
Li Y, Huang J, Ji M, Ran J. 2015. Dryland expansion in Northern China from 1948 to 2008. Adv Atmos Sci, 32: 870–876
Lu J, Delworth T L. 2005. Oceanic forcing of the late 20th century Sahel drought. Geophys Res Lett, 32: L22706
Lyon B. 2004. The strength of El Niño and the spatial extent of tropical drought. Geophys Res Lett, 31: L21204
Maestre F T, Escolar C, de Guevara M L, Quero J L, Lázaro R, Delgado-Baquerizo M, Ochoa V, Berdugo M, Gozalo B, Gallardo A. 2013. Changes in biocrust cover drive carbon cycle responses to climate change in drylands. Glob Change Biol, 19: 3835–3847
Ma Z G. 2007. The interdecadal trend and shift of dry/wet over the central part of North China and their relationship to the Pacific Decadal Oscillation (PDO). Chin Sci Bull, 52: 2130–2139
Ma Z G, Fu C B. 2003. Interannual characteristics of the surface hydrological variables over the arid and semi-arid areas of Northern China. Global Planet Change, 37: 189–200
Ma Z, Fu C. 2006. Some evidence of drying trend over northern China from 1951 to 2004. Chin Sci Bull, 51: 2913–2925
Ma Z G, Fu C B. 2007. Evidences of drying trend in the global during the latter half of 20th century and their relationship with large scale climate background. Sci China Earth Sci, 50: 776–788
Ma Z G, Shao L J. 2006. Relationship between dry/wet variation and the Pacific decadal oscillation (PDO) in northern China during the last 100 years. Chin J Atmos Sci, 30: 464–474
Mantua N J, Hare S R, Zhang Y, Wallace J M, Francis R C. 1997. A Pacific interdecadal climate oscillation with impacts on salmon production. Bull Amer Meteorol Soc, 78: 1069–1079
Mantua N J, Hare S R. 2002. The Pacific decadal oscillation. J Oceanogr, 58: 35–44
McCabe G J, Palecki M A, Betancourt J L. 2004. Pacific and Atlantic Ocean influences on multidecadal drought frequency in the United States. Proc Natl Acad Sci USA, 101: 4136–4141
Mo K C, Schemm J K E, Yoo S H. 2009. Influence of ENSO and the Atlantic multidecadal oscillation on drought over the United States. J Clim, 22: 5962–5982
Narisma G T, Foley J A, Licker R, Ramankutty N. 2007. Abrupt changes in rainfall during the twentieth century. Geophys Res Lett, 34: L06710
Nicholson S E, Tucker C J, Ba M B. 1998. Desertification, drought, and surface vegetation: An example from the West African Sahel. Bull Amer Meteorol Soc, 79: 815–829
Nicholson S E, Some B, Kone B. 2000. An analysis of recent rainfall conditions in West Africa, including the rainy seasons of the 1997 El Niño and the 1998 La Niña years. J Clim, 13: 2628–2640
Nicholson S E, Grist J P. 2001. A conceptual model for understanding rainfall variability in the West African Sahel on interannual and interdecadal timescales. Int J Climatol, 21: 1733–1757
Nitta T. 1986. Long-term variations of cloud amount in the western Pacific region. J Meteorol Soc Jpn, 64: 373–390
Nitta T. 1987. Convective activities in the tropical western Pacific and their impact on the Northern Hemisphere summer circulation. J Meteorol Soc Jpn, 65: 373–390
Rietkerk M, Dekker S C, de Ruiter P C, van de Koppel J. 2004. Self-organized patchiness and catastrophic shifts in ecosystems. Science, 305: 1926–1929
Qian C, Zhou T J. 2014. Multidecadal variability of North China aridity and its relationship to PDO during 1900–2010. J Clim, 27: 1210–1222
Rasmusson E M, Arkin P A. 1993. A global view of large-scale precipitation variability. J Clim, 6: 1495–1522
Reynolds J F, Smith D M S, Lambin E F, Turner B L, Mortimore M, Batterbury S P J, Downing T E, Dowlatabadi H, Fernández R J, Herrick J E, Huber-Sannwald E, Jiang H, Leemans R, Lynam T, Maestre F T, Ayarza M, Walker B. 2007. Global desertification: Building a science for dryland development. Science, 316: 847–851
Rogers J C. 1984. The association between the North Atlantic oscillation and the Southern oscillation in the Northern hemisphere. Mon Weather Rev, 112: 1999–2015
Ropelewski C F, Halpert M S. 1987. Global and regional scale precipitation patterns associated with the El Niño/Southern oscillation. Mon Weather Rev, 115: 1606–1626
Scheffer M, Carpenter S, Foley J A, Folke C, Walker B. 2001. Catastrophic shifts in ecosystems. Nature, 413: 591–596
Schubert S, Gutzler D, Wang H, Dai A, Delworth T, Deser C, Findell K, Fu R, Higgins W, Hoerling M, Kirtman B, Koster R, Kumar A, Legler D, Lettenmaier D, Lyon B, Magana V, Mo K, Nigam S, Pegion P, Phillips A, Pulwarty R, Rind D, Ruiz-Barradas A, Schemm J, Seager R, Stewart R, Suarez M, Syktus J, Ting M, Wang C, Weaver S, Zeng N. 2009. A US CLIVAR project to assess and compare the responses of global climate models to drought-related SST forcing patterns: Overview and results. J Clim, 22: 5251–5272
Seager R, Naik N, Baethgen W, Robertson A, Kushnir Y, Nakamura J, Jurburg S. 2010. Tropical oceanic causes of interannual to multidecadal precipitation variability in Southeast South America over the past century. J Clim, 23: 5517–5539
Shukla J, Wallace J M. 1983. Numerical simulation of the atmospheric response to equatorial Pacific sea surface temperature anomalies. J Atmos Sci, 40: 1613–1630
Shi Y F, Shen Y P, Hu R J. 2002. Preliminary study on signal, impact and foreground of climatic shift from warm-dry to warm-humid in Northwest China (in Chinese). J Glaciol Geocryol, 24: 219–226
Si D, Ding Y. 2016. Oceanic forcings of the interdecadal variability in East Asian summer rainfall. J Clim, 29: 7633–7649
Spinoni J, Vogt J, Naumann G, Carrao H, Barbosa P. 2015. Towards identifying areas at climatological risk of desertification using the Köppen-Geiger classification and FAO aridity index. Int J Climatol, 35: 2210–2222
Straus D M, Shukla J. 2002. Does ENSO force the PNA? J Clim, 15: 2340–2358
Sutton R T, Hodson D L R. 2005. Atlantic Ocean forcing of North American and European summer climate. Science, 309: 115–118
Ting M, Wang H. 1997. Summertime U.S. precipitation variability and its relation to Pacific Sea surface temperature. J Clim, 10: 1853–1873
Ting M F, Kushnir Y, Seager R, Li C H. 2011. Robust features of Atlantic multi-decadal variability and its climate impacts. Geophys Res Lett, 38: 351–365
Trenberth K. 2011. Changes in precipitation with climate change. Clim Res, 47: 123–138
Trenberth K E, Branstator G W, Karoly D, Kumar A, Lau N C, Ropelewski C. 1998. Progress during TOGA in understanding and modeling global teleconnections associated with tropical sea surface temperatures. J Geophys Res, 103: 14291–14324
Trenberth K E, Dai A, van der Schrier G, Jones P D, Barichivich J, Briffa K R, Sheffield J. 2014. Global warming and changes in drought. Nat Clim Change, 4: 17–22
Trenberth K E, Hurrell J W. 1994. Decadal atmosphere-ocean variations in the Pacific. Clim Dyn, 9: 303–319
White R P, Nackoney J. 2003. Drylands, People and Ecosystem Goods and Services. Washington: World Resources Institute
Wang B, Wu R G, Fu X H. 2000. Pacific-East Asian teleconnection: How does ENSO affect East Asian climate? J Clim, 13: 1517–1536
Wang L, Huang G, Chen W, Zhou W, Wang W Q. 2018. Wet-to-dry shift over Southwest China in 1994 tied to the warming of tropical warm pool. Clim Dyn, 51: 3111–3123
Wang S W, Zhu J H. 1999. A review of overseas study on interdecadal variability (in Chinese). Acta Meteorol Sin, 57: 376–384

Wu G X, Liu Y M, Wang T M, Wan R J, Liu X, Li W P, Wang Z Z, Zhang Q, Duan A M, Liang X Y. 2007. The influence of mechanical and thermal forcing by the Tibetan Plateau on Asian climate. J Hydrometeorol, 8: 770–789

Wu G X, Liu Y M, Yu J J, Zhu X Y, Ren R C. 2008. Modulation of land-sea distribution on air-sea interaction and formation of subtropical anticyclones. Chin J Atmos Sci, 32: 720–740

Wu R G, Chen L T. 1992. Interannual variation of the PNA flow pattern and impacts of extratropical and tropical SSTs (in Chinese). Chin J Atmos Sci, 16: 583–591

Xie S P, Hu K, Hafner J, Tokinaga H, Du Y, Huang G, Sampe T. 2009. Indian Ocean capacitor effect on Indo-Western Pacific climate during the summer following El Niño. J Clim, 22: 730–747

Xie S P, Kosaka Y, Du Y, Hu K, Chowdary J S, Huang G. 2016. Indo-western Pacific Ocean capacitor and coherent climate anomalies in post-ENSO summer: A review. Adv Atmos Sci, 33: 411–432

Xu B L. 2016. The Variation Characteristics of Global and Regional Land Precipitation on Multiple Time Scale and Their Relationship with SST (in Chinese). Beijing: Chinese Academy of Sciences

Xu B L, Ma Z G. 2017. Decadal characteristics of global land annual precipitation variation on multiple spatial scales (in Chinese). Chin J Atmos Sci, 41: 593–602

Yan Z W, Ji J J, Ye D Z. 1990. Summer climatic jump in northern hemisphere during the 1960s I: Precipitatipn and temperature (in Chinese). Sci China Earth Sci, 1: 97–103

Yang F, Lau K M. 2004. Trend and variability of China precipitation in spring and summer: Linkage to sea-surface temperatures. Int J Climatol, 24: 1625–1644

Yang Q, Ma Z G, Fan X G, Yang Z L, Xu Z F, Wu P L. 2017. Decadal modulation of precipitation patterns over Eastern China by sea surface temperature anomalies. J Clim, 30: 7017–7033

Zhang R, Delworth T L. 2006. Impact of Atlantic multidecadal oscillations on India/Sahel rainfall and Atlantic hurricanes. Geophys Res Lett, 33: L17712

Zhang Q Y, Chen L T. 1991. Variations of dryness and wetness in China during 1951–1980 (in Chinese). Chin J Atmos Sci, 15: 72–81

Zhou L, Chen H, Hua W, Dai Y, Wei N. 2016. Mechanisms for stronger warming over drier ecoregions observed since 1979. Clim Dyn, 47: 2955–2974

Zhu Y L, Wang T, Ma J H. 2016. Influence of internal decadal variability on the summer rainfall in Eastern China as simulated by CCSM4. Adv Atmos Sci, 33: 706–714

(Responsible editor: Wen CHEN)